ISBN: 978-3-95450-208-0 doi:10.18429/JACoW-IPAC2019-WEPTS015

SYNCHRONOUS MEASUREMENTS OF ELECTRON BUNCHES UNDER THE INFLUENCE OF THE MICROBUNCHING INSTABILITY

M. Brosi*, T. Boltz, E. Bründermann, S. Funkner, B. Kehrer, M. J. Nasse, G. Niehues, M. M. Patil, P. Schönfeldt†, P. Schreiber, J. L. Steinmann and A.-S. Müller,
Karlsruhe Institute of Technology, Karlsruhe, Germany

Abstract

The microbunching instability is a longitudinal collective instability which occurs for short electron bunches in a storage ring above a certain threshold current. The instability leads to a charge modulation in the longitudinal phase space. The resulting substructures on the longitudinal bunch profile vary over time and lead to fluctuations in the emitted power of coherent synchrotron radiation (CSR). To study the underlying longitudinal dynamics on a turn-by-turn basis, the KIT storage ring KARA (Karlsruhe Research Accelerator) provides a wide variety of diagnostic systems. By synchronizing the single-shot electro-optical spectral decoding setup (longitudinal profile), the bunch-by-bunch THz detection systems (THz power) and the horizontal bunch size measurement setup (energy spread), three important properties of the bunch during this instability can be measured at every turn for long time scales. This allows a deep insight into the dynamics of the bunch under the influence of the microbunching instability. This contribution will discuss effects like the connection between the emitted CSR power and the deformations in the longitudinal bunch profile on the time scale of the instability.

INTRODUCTION

The KIT storage ring KARA (Karlsruhe Research Accelerator) provides a short-bunch operation mode with a reduced momentum compaction factor to achieve bunch lengths in the order of picoseconds [1, 2]. At this operation mode the microbunching instability can be observed. This longitudinal instability occurs due to the self-interaction of the electron bunch with its own coherent synchrotron radiation (CSR). The shorter the bunch the higher the frequencies up to which CSR is emitted and the stronger the effect of the microbunching instability. The behavior of the bunch under the influence of the instability changes depending on different parameters such as bunch current, momentum compaction factor, and RF voltage [3, 4].

BEAM DYNAMICS

In general the microbunching instability results in substructures in the longitudinal phase space. These arise as soon as the bunch is short enough so that its form factor has a significant overlap with the involved impedances. As simplified model of the CSR impedance, the parallel plates model was proven to fit quite well to the experimental results at KARA [4].

The overlap of the form factor with the impedance in frequency domain causes an additional wake potential and with this a deformation of the bunch [5]. At low currents this manifests in an asymmetric longitudinal bunch profile (given by the Haissinski solution [6]). The deformation leads to even higher frequency components in the form factor and therefore an even stronger additional wake potential. This self-interaction will increase and result in stronger deformations the higher the bunch current becomes.

At a certain current value the instability threshold is reached and the deformations form finger-like substructures on the charge distribution in the longitudinal phase space, now also affecting the energy distribution. At this point the bunch profile is not constant anymore, as the substructures rotate with the distribution in the phase space. These fast changes in the longitudinal profile lead directly to changes in the emitted CSR spectrum and therefore fluctuations in the emitted CSR power [7].

For even higher currents an additional slowly repeating behavior can be observed. The self-interaction leads to a growth of the substructures, which after some synchrotron periods, are being washed out by diffusion and filamentation. This results in an increased bunch size and therefore a lower wake potential. At this point, the radiation damping outweighs the driving wake potential, the substructures dissolve and the overall bunch length is damped down to the point, where the wake potential increases and leads again to the formation of substructures.

To simulate the influence of the instability on the bunch, the Vlasov-Fokker-Planck solver Inovesa [8, 9], was developed at KIT. For each time step, the simulation calculates the wake potential from the CSR impedance and the longitudinal bunch profile. The resulting kick is applied to the charge distribution in phase space altering the distribution for the next step. As the simulation operates in phase space, it provides direct insight into the dynamics under the instability.

MEASUREMENT

From the experimental side, a direct measurement of the longitudinal phase space distribution is not feasible. Therefore, the projection on the time as well as the projection on the energy axis are measured. Additionally, the emitted CSR power is measured, which is directly connected to the bunch profile and the CSR impedance. The experimental setups present at KARA allow for on-turn synchronized observation as demonstrated in [10, 11].

* miriam.brosi@kit.edu
† now at DLR-VE, Oldenburg, Germany

ISBN: 978-3-95450-208-0 doi:10.18429/JACoW-IPAC2019-WEPTS015

Coherent Synchrotron Radiation

For the emitted CSR in the THz range, fast room-temperature Schottky barrier diodes [12, 13], sensitive from 50 GHz up to 1 THz are combined with KAPTURE [14, 15]. The newest version, KAPTURE-2 [16], consists of eight readout channels, each with a 18 GHz track-and-hold unit and a 12-bit 1 GHz ADC. KAPTURE allows to measure all bunches simultaneously. For the following measurement, a waveguide-coupled Schottky diodes (220 GHz - 325 GHz) was used. As the measurements were conducted in single-bunch operation a 4 GHz oscilloscope was used in parallel.

Longitudinal Bunch Profile

The longitudinal bunch profile is measured with an electro-optical near-field setup [17, 18]. For this, a chirped laser pulse is sent through an electro-optical crystal at the same time the bunch passes close by. In combination with a fast spectrometer, turn-by-turn single-shot profiles can be measured. This is achieved with a grating and the line array detector KALYPSO [19, 20]. KALYPSO III is under development and will provide up to 10 Mfps with 512 pixels [21].

Horizontal Bunch Size

The energy spread of the bunch is correlated via the dispersion, the emittance, and the beta function with the horizontal bunch size. Hence, the horizontal bunch profile is detected at the Visible Light Diagnostics port [22], in a dispersive region of the storage ring, with the fast line array detector KALYPSO at each turn continuously [11, 23, 24]. The changes occurring in the horizontal bunch size estimated from the measured profile are used as an indication for the changes in the energy spread.

Synchronization

The synchronization of the detector systems can be checked by triggered jumps in the RF phase, which are visible as onset of strong synchrotron oscillations [10]. Even during undisturbed operation the synchrotron oscillation amplitude changes significantly, which can be seen in Fig. 1 in the measured bunch length and longitudinal position as well as in the horizontal size and position. This served as intrinsic check of the synchronization.

Analysis

The calculation of the derived parameters like size (length) and center of mass position (phase) from the measured horizontal and longitudinal profiles is done in post processing. Due to the deformation of the bunch caused by the instability, the bunch shape is not Gaussian any more and even varies with time. While the horizontal position is determined from the first statistical moment (center of mass) of the individual profile, for the longitudinal position the position of the maximum is taken as a measure (due to a slightly tilted base line). For the bunch length and the horizontal size, the standard deviation is calculated. This has to be taken into account when interpreting the results.

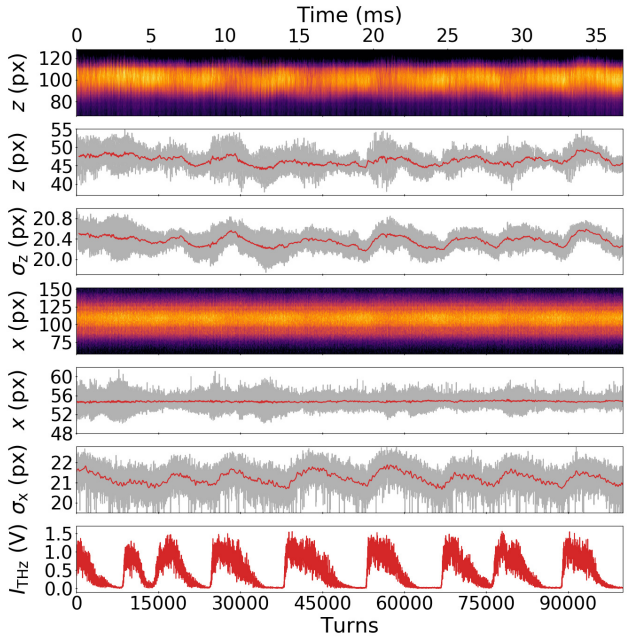

Figure 1: Synchronized measurement. From top to bottom: longitudinal profile, longitudinal position, longitudinal bunch length, horizontal profile, horizontal position, horizontal size and THz intensity. For panel 2, 3, 5, and 6 in grey synchrotron oscillation (and noise) around slowly changing average (red).

RESULTS

Measurement

In the measurement (Fig. 1) a sawtooth shaped pattern formed by the increase and following decrease of the bunch length as well as the horizontal bunch size can be seen over several thousand turns. The repetition rate is consistent with the one visible in the bursts of emitted CSR. Between turn number 7500 and 22500 (Fig. 1) two shorter bursts occur in the CSR emission. These are also visible in the length and horizontal size, showing the link between the changes in bunch size and the emitted CSR power.

Figure 2 shows a short time range around the onset of a CSR burst. Around turn 24700 ($\approx$ 9.1 ms), where the emitted CSR power starts to increase significantly, substructures on the longitudinal bunch profile start to form. After approximately 2.5 to 3 synchrotron periods (at approx. turn 25300 $\approx$ 9.3 ms) they start to be less pronounced and begin to wash out. While the bunch length (STD of the bunch profile) starts to increase approximately at the same time the substructures occur, the horizontal bunch size (corresponding to the energy spread) seems to stay constant at a low value until the substructures start to wash out. Similar results are reported in [24].

The observed behavior fits to the expectations described in the beam dynamics section. The occurrence of the substructures on the longitudinal phase space and therefore bunch profile leads directly to an increase in the emitted CSR power. This drives the self-amplification of the substructures via the wake potential until they are washed out by filamenta-

ISBN: 978-3-95450-208-0 doi:10.18429/JACoW-IPAC2019-WEPTS015

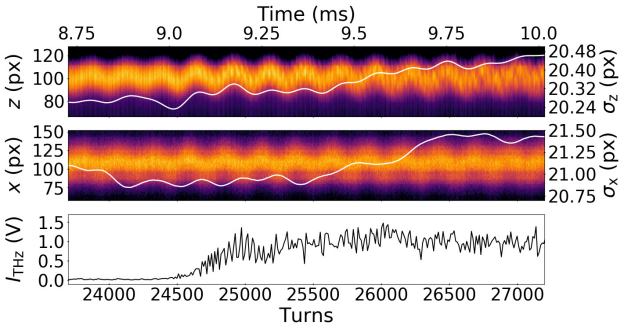

Figure 2: Zoom-in of Fig. 1 to onset of CSR burst. Long. and hor. size as white lines on corresponding profiles.

tion. The calculation of the standard deviation of the profile (bunch length) is sensitive to the occurrence of these substructures and therefore a first increase of the bunch length is observed. No substructures are visible on the measured horizontal profile. This could be due to the diffraction limit of the optical beam path and the fact, that the horizontal size also contains a contribution from the emittance. So, the horizontal size remains constant until the substructures filament out and increase the overall size in phase space and consequently the energy spread. The washed out and blown up distribution in phase space is then damped down, leading to the decrease in bunch length as well as energy spread.

The increased CSR emission during a burst is also visible in the longitudinal position of the bunch (position of maxima in longitudinal bunch profile) in Fig. 1. The bunch moves to a slightly different phase of the acceleration voltage to compensate for the increase in radiation loss. However, the additional radiation loss is small (in the order of 1 keV) compared to the radiation loss due to incoherent synchrotron radiation (46 keV). This effect can not be resolved in the horizontal position (≃ energy mismatch via dispersion) and the initial energy mismatch is compensated by the bunch moving to a different phase, where it gains the necessary additional energy in the RF cavities.

The phase shift could trigger the onset of synchrotron oscillations around the new phase. In the measurements no correlation is visible between changes of the synchrotron oscillation amplitude (visible e.g. on the horizontal bunch position (grey curve in 5th panel of Fig. 1)) and the state of the CSR bursts. This is not unexpected as the synchrotron oscillation is strongly driven by RF phase noise [25].

Simulation

In Fig. 3 simulation results by Inovesa are similarly displayed to the measurements in Fig. 1 and Fig. 2. In contrast to the measurements, some structures are always visible on the longitudinal as well as the energy profile. As soon as the substructures become prominent, the emitted CSR power increases and at the same time the bunch length as well as the energy spread start to grow. The simultaneous increase in length and energy spread supports the hypothesis that the delayed increase of the measured horizontal size could be attributed to the observation, that the substructures are not

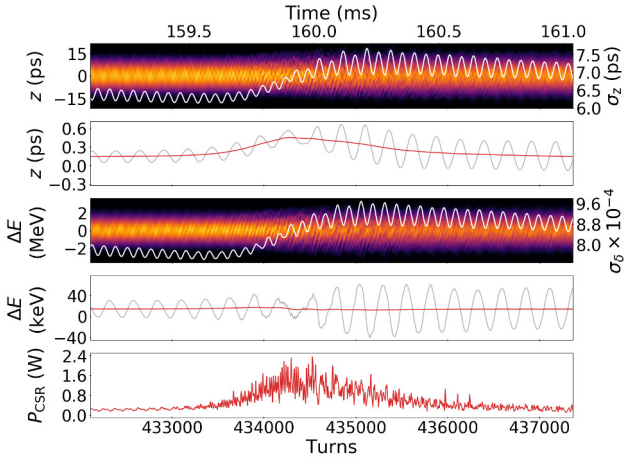

Figure 3: Simulation results displayed similarly to Fig.1. For panel 2 and 4 a moving average is displayed in red.

visible on the measured horizontal profile. The simulation also shows, that the substructures are washed out, which is followed by a damping of the overall size.

Additionally, the simulation shows a small shift in the longitudinal position (phase) of the bunch during the increased CSR emission. Figure 3 (2nd panel from top) shows that this shift in phase is in the order of the amplitude of the synchrotron oscillation. The change on the mean energy deviation is significantly smaller than the synchrotron oscillation amplitude. It is more in the order of 1 keV, which corresponds to the estimated energy loss due to the increased CSR emission. In the simulations the excitation by RF noise is missing [26], thus a change in synchrotron oscillation amplitude caused by the phase shift is visible.

CONCLUSION

In the presented measurements, the effect of the microbunching instability is visible in the longitudinal and horizontal plane as well as in the emitted CSR power. The synchronization of the measurements allows to study the connection between the different parameters. The discussed features are also present in the simulation results. Small deviations between the behavior in the measurement and the simulation, like the difference in the onset of the increase of the horizontal bunch size (≃ energy spread), could be attributed to the fact, that some parameters can only be indirectly obtained with the presented measurement setup.

ACKNOWLEDGEMENTS

This work has been supported by the German Federal Ministry of Education and Research (Grant No. 05K16VKA). MB, PS, and JLS acknowledge the support by the Helmholtz International Research School for Teratronics.

REFERENCES

[1] A.-S. Müller *et al.*, "Far Infrared Coherent Synchrotron Edge Radiation at ANKA", in *Proc. 21st Particle Accelerator Conf. (PAC'05)*, Knoxville, TN, USA, May 2005, paper RPAE038.

ISBN: 978-3-95450-208-0 doi:10.18429/JACoW-IPAC2019-WEPTS015

[2] M. Klein *et al.*, "Modeling the Low-Alpha-Mode at ANKA with the Accelerator Toolbox", in *Proc. 24th Particle Accelerator Conf. (PAC'11)*, New York, NY, USA, Mar.-Apr. 2011, paper WEP005, pp. 1510–1512.

[3] K. L. F. Bane, Y. Cai, and G. Stupakov, "Threshold studies of the microwave instability in electron storage rings", *Phys. Rev. ST Accel. Beams*, vol. 13, p. 104402, Oct. 2010. doi:10.1103/PhysRevSTAB.13.104402

[4] M. Brosi *et al.*, "Fast mapping of terahertz bursting thresholds and characteristics at synchrotron light sources", *Phys. Rev. Accel. Beams*, vol. 19, p. 110701, Nov. 2016. doi:10.1103/PhysRevAccelBeams.19.110701

[5] T. Boltz *et al.*, "Perturbation of Synchrotron Motion in the Micro-Bunching Instability", presented at the 10th Int. Particle Accelerator Conf. (IPAC'19), Melbourne, Australia, May 2019, paper MOPGW018, this conference.

[6] J. Haïssinski, "Exact longitudinal equilibrium distribution of stored electrons in the presence of self-fields", *J. Nuov Cim B*, vol. 18, p. 72, Nov. 73. https://link.springer.com/article/10.1007/BF02832640

[7] J. L. Steinmann *et al.*, "Continuous bunch-by-bunch spectroscopic investigation of the microbunching instability", *Phys. Rev. Accel. Beams*, vol. 21, p. 110705, Nov. 2018. doi:10.1103/PhysRevAccelBeams.21.110705

[8] P. Schönfeldt *et al.*, "Parallelized Vlasov-Fokker-Planck solver for desktop personal computers", *Phys. Rev. Accel. Beams*, vol. 20, p. 030704, Mar. 2017. doi:10.1103/PhysRevAccelBeams.20.030704

[9] Schönfeldt, Patrik et al.: Inovesa/Inovesa: Gamma Two. (2018), Jul. http://dx.doi.org/10.5281/zenodo.1321580.

[10] B. Kehrer *et al.*, "Synchronous detection of longitudinal and transverse bunch signals at a storage ring", *Phys. Rev. Accel. Beams*, vol. 21, p. 102803, Oct. 2018. doi:10.1103/PhysRevAccelBeams.21.102803

[11] J. L. Steinmann *et al.*, "Turn-by-Turn Measurements for Systematic Investigations of the Micro-Bunching Instability", in *Proc. 60th ICFA Advanced Beam Dynamics Workshop on Future Light Sources (FLS'18)*, Shanghai, China, Mar. 2018, pp. 46–51. doi:10.18429/JACoW-FLS2018-TUP2WD03

[12] ACST GmbH, http://www.acst.de/

[13] Virginia Diodes, Inc., http://vadiodes.com/

[14] M. Caselle *et al.*, "An ultra-fast data acquisition system for coherent synchrotron radiation with terahertz detectors", *J. Instrum.*, vol. 9, p. C01024, Jan. 2014. doi:10.1088/1748-0221/9/01/C01024

[15] C. M. Caselle *et al.*, "Commissioning of an Ultra-fast Data Acquisition System for Coherent Synchrotron Radiation Detection", in *Proc. 5th Int. Particle Accelerator Conf. (IPAC'14)*, Dresden, Germany, Jun. 2014, pp. 3497–3499. doi:10.18429/JACoW-IPAC2014-THPME113

[16] M. Caselle *et al.*, "KAPTURE-2. A picosecond sampling system for individual THz pulses with high repetition rate", *J. Instrum.*, vol. 12, p. C01040, Jan. 2017. doi:10.1088/1748-0221/12/01/c01040

[17] N. Hiller *et al.*, "A Setup for Single Shot Electro Optical Bunch Length Measurements at the ANKA Storage Ring", in *Proc. 2nd Int. Particle Accelerator Conf. (IPAC'11)*, San Sebastian, Spain, Sep. 2011, paper TUPC086, pp. 1206–1208.

[18] S. Funkner *et al.*, "High throughput data streaming of individual longitudinal electron bunch profiles", *Phys. Rev. Accel. Beams*, vol. 22, p. 022801, Feb. 2019. doi:10.1103/PhysRevAccelBeams.22.022801

[19] L. Rota *et al.*, "KALYPSO: A Mfps Linear Array Detector for Visible to NIR Radiation", in *Proc. 5th Int. Beam Instrumentation Conf. (IBIC'16)*, Barcelona, Spain, Sep. 2016, pp. 740–743. doi:10.18429/JACoW-IBIC2016-WEPG46

[20] L. Rota *et al.*, "KALYPSO: Linear array detector for high-repetition rate and real-time beam diagnostics", *Nucl. Instrum. Methods Phys. Res., Sect. A*, Oct. 2018, in press 10.1016/j.nima.2018.10.093

[21] M. M. Patil *et al.*, "An Ultra-Fast and Wide-Spectrum Linear Array Detector for High Repetition Rate and Pulsed Experiments", presented at the 10th Int. Particle Accelerator Conf. (IPAC'19), Melbourne, Australia, May 2019, paper WEPGW018, this conference.

[22] B. Kehrer *et al.*, "Visible Light Diagnostics at the ANKA Storage Ring", in *Proc. 6th Int. Particle Accelerator Conf. (IPAC'15)*, Richmond, VA, USA, May 2015, pp. 866–868. doi:10.18429/JACoW-IPAC2015-MOPHA037

[23] B. Kehrer *et al.*, "Time-Resolved Energy Spread Studies at the ANKA Storage Ring", in *Proc. 8th Int. Particle Accelerator Conf. (IPAC'17)*, Copenhagen, Denmark, May 2017, pp. 53–56. doi:10.18429/JACoW-IPAC2017-MOOCB1

[24] B. Kehrer *et al.*, "Turn-by-Turn Horizontal Bunch Size and Energy Spread Studies at KARA", presented at the 10th Int. Particle Accelerator Conf. (IPAC'19), Melbourne, Australia, May 2019, paper WEPGW016, this conference.

[25] W. Ormond and T. Rogers, "Synchrotron Oscillation Driven by RF Phase Noise", in *Proc. 17th Particle Accelerator Conf. (PAC'97)*, Vancouver, Canada, May 1997, paper 4V038, pp.1822–1824. doi:10.1109/PAC.1997.751029

[26] P. Schönfeldt *et al.*, "Elaborated Modeling of Synchrotron Motion in Vlasov-Fokker-Planck Solvers", *J. Phys. Conf. Ser.*, vol. 1067, p. 062025, Sep. 2018. doi:10.1088/1742-6596/1067/6/062025